JACS
JOURNAL OF THE AMERICAN CHEMICAL SOCIETY
pubs.acs.org/JACS
Article

Enantioselective Synthesis of Chiral β^2-Amino Phosphorus Derivatives via Nickel-Catalyzed Asymmetric Hydrogenation

Hanlin Wei, Yicong Luo, Jinhui Li, Jianzhong Chen,* Ilya D. Gridnev,* and Wanbin Zhang*

Cite This: https://doi.org/10.1021/jacs.4c10623
Read Online
ACCESS | Metrics & More | Article Recommendations | Supporting Information

ABSTRACT: Compared with chiral β^3-amino phosphorus compounds, which can be easily derived from natural optically pure α-amino acids, obtaining chiral β^2-amino phosphorus derivatives remains a challenge. These derivatives, which cannot be derived from chiral natural amino acids, possess unique biological activities or potential catalytic activities. Herein, highly enantioselective hydrogenation for the preparation of chiral β^2-amino phosphorus derivatives from *E*-β-enamido phosphorus compounds is reported by using a green and low-cost earth-abundant metal nickel catalyst (13 examples of 99% ee). In particular, this catalytic system provides the same enantiomer product from the *E*- and *Z*-alkene substrates, and the *E*/*Z*-substrate mixtures provide good results (up to 96% ee). The products can be diversely derivatized, and the derivatives exhibit good catalytic activities as novel chiral β^2-aminophosphine ligands. Density functional theory calculations reveal that the weak attractive interactions between the nickel catalyst and the substrate are crucial for achieving perfect enantioselectivities. In addition, the different coordination modes between the *E*- or *Z*-substrates and the catalyst may result in the formation of the same enantiomer product.

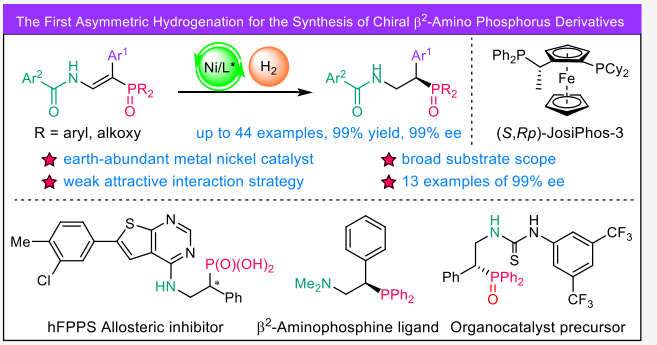

INTRODUCTION

Chiral β-amino phosphonic acids and their derivatives are widely used in medicines and pesticides because of the high biological activities of both the N and P groups (Scheme 1A, top).[1,2] For instance, replacing natural chiral amino acids in proteins with corresponding amino phosphonic acids leads to significant alterations in protein structures and properties. Consequently, this modification opens up potential new drug applications in biochemical and physiological processes.[2] In addition, chiral β-aminophosphine derivatives are also recognized as effective chiral P,N ligands and organocatalysts in asymmetric catalytic reactions because the N and P groups can be modified sterically and electronically, respectively (Scheme 1A, bottom).[3] However, in contrast to β^3-amino phosphorus compounds, which can be derived from natural sources,[3b] β^2-amino phosphorus derivatives cannot be synthesized from chiral natural amino acids (Scheme 1B). This poses greater challenges in their preparation, resulting in a significant lack of such chiral molecules in practical applications.

To date, a few studies have successfully achieved the asymmetric synthesis of β^2-amino phosphorus derivatives through Michael additions or hydrophosphination reactions of P(O)−H or P−H groups with nitroalkenes, respectively.[4] However, more efficient, convenient, and greener methods for the asymmetric catalytic synthesis of such chiral molecules are scarce and need further development.

Catalytic asymmetric hydrogenation has received significant attention in the past few decades due to its high catalytic efficiency and atom economy.[5] The synthesis of chiral β^3- and $\beta^{2,3}$-amino phosphorus derivatives by noble metal (Rh and Ir)-catalyzed asymmetric hydrogenation has been studied, and many excellent results have been achieved (Scheme 1C).[6] However, the synthesis of β^2-amino phosphorus derivatives by asymmetric hydrogenation has not been reported. As commonly recognized, the electronic properties of P and N substituents on olefins contribute to the low hydrogenation activity of β-enamido phosphorus substrates. Additionally, the mixture of the *E*/*Z* configuration and their isomerization further complicates matters. Typically, the enantioselectivities of asymmetric hydrogenation with *E*- and *Z*-substrates differ, generally resulting in opposite enantiomers. Consequently, achieving high enantioselectivity with *E*- and *Z*-enamides under the same catalytic conditions proves challenging.[7]

In recent years, there has been an increasing demand for the development of asymmetric hydrogenation reactions with

Received: August 3, 2024
Revised: December 13, 2024
Accepted: December 17, 2024

Scheme 1. β-Amino Phosphorus Derivatives and Their Synthesis Methods

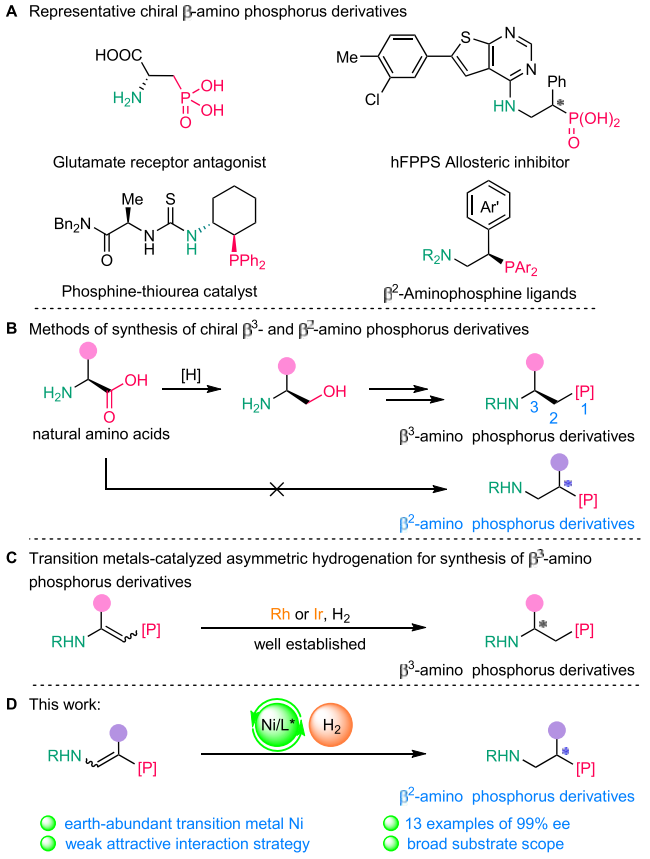

cheap and readily available earth-abundant metals as catalysts.[8−15] As one of the earth-abundant metals, nickel has shown excellent catalytic potential due to its inherent characteristics in this field.[8d,f,10−15] Many excellent studies regarding Ni-catalyzed asymmetric hydrogenation have been reported by Hamada,[10] Zhou,[11] Chirik,[12] Zhang,[13] our group,[14] and other research groups.[15] In recent years, we reported the asymmetric hydrogenations of α-substituted vinyl phosphorus derivatives, *E*/*Z*-imine, and enamide substrates using nickel catalytic systems, in which the weak attractive interactions between the Ni catalyst and substrate play key roles in improving reactivities and generating high enantioselectivities.[14b,c,e,f] Herein, we report highly enantioselective Ni-catalyzed hydrogenation of *E*-β-enamido phosphine oxide, *E*-β-enamido phosphonate, and *E*/*Z*-β-enamido phosphine oxide substrates based on the weak attractive interaction strategy (Scheme 1D).

RESULTS AND DISCUSSION

Hydrogenation was initiated by exploring the chiral diphosphine ligands using *E*-*N*-(2-(diphenylphosphoryl)-2-phenylvinyl)benzamide (*E*-**1a**) as a model substrate (Table 1). With (*R*)-SegPhos (5.0 mol %) as the ligand, $Ni(OAc)_2 \cdot 4H_2O$ (5.0 mol %) as the nickel source, and TFE (2,2,2-trifluoroethanol) as the solvent, the reaction was not successful under 40 bar H_2 at 80 °C over 24 h (entry 1). Changing (*R*)-SegPhos to its highly substituted phenyl ring analogue (*R*)-DTBM-SegPhos, whose eight *t*-butyl groups can usually produce weak attractive interactions with the substrate, the conversion increased to 11% (entry 2). The more electron-rich

Table 1. Optimization of the Reaction Conditions[a]

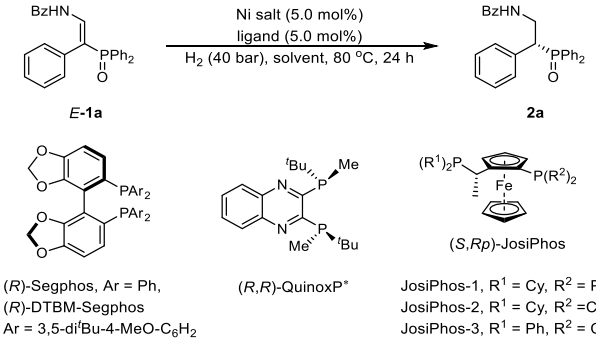

entry	Ni salt	ligand	sol.	conv. (%)[b]	ee (%)[c]
1	$Ni(OAc)_2 \cdot 4H_2O$	(*R*)-SegPhos	TFE	<5	
2	$Ni(OAc)_2 \cdot 4H_2O$	(*R*)-DTBM-SegPhos	TFE	11	
3	$Ni(OAc)_2 \cdot 4H_2O$	(*R*,*R*)-QuinoxP*	TFE	<5	
4	$Ni(OAc)_2 \cdot 4H_2O$	(*S*,*Rp*)-JosiPhos-1	TFE	>99	80
5	$Ni(OAc)_2 \cdot 4H_2O$	(*S*,*Rp*)-JosiPhos-2	TFE	13	-
6	$Ni(OAc)_2 \cdot 4H_2O$	(*S*,*Rp*)-JosiPhos-3	TFE	27	97
7	$Ni(ClO_4)_2 \cdot 6H_2O$	(*S*,*Rp*)-JosiPhos-3	TFE	74	97
8	$Ni(OTf)_2$	(*S*,*Rp*)-JosiPhos-3	TFE	80	97
9	$Ni(OTf)_2$	(*S*,*Rp*)-JosiPhos-3	HFIP	89	99
10[d]	$Ni(OTf)_2$	(*S*,*Rp*)-JosiPhos-3	HFIP	>99	99

[a]Reaction conditions: **1a** (0.10 mmol), $Ni(OAc)_2 \cdot 4H_2O$ (5.0 mol %), ligand (5.0 mol %), TFE (1.5 mL), H_2 (40 bar), 80 °C, 24 h. [b]The conversions were calculated from ^1H NMR spectra. [c]The *ee* values were determined by HPLC using chiral columns. [d]$Ni(OTf)_2$ (7.5 mol %), (*S*,*Rp*)-JosiPhos-3 (5.0 mol %), M/L = 1.5/1. TFE = 2,2,2-trifluoroethanol, HFIP = 1,1,1,3,3,3-hexafluoro-2-propanol.

P-chiral ligand (*R*,*R*)-QuinoxP*, commonly used in nickel catalysts, did not provide any of the desired products (entry 3). To our delight, when using the electron-rich chiral ligand (*S*,*Rp*)-JosiPhos-1, the reaction afforded good enantioselectivity and excellent reactivity (>99% conversion, 80% ee, entry 4). Further screening of (*S*,*Rp*)-JosiPhos-2 and (*S*,*Rp*)-JosiPhos-3 with different substituents (entries 5 and 6) showed that the latter produced the desired product with excellent enantioselectivity (97% ee) but only 27% conversion. This result prompted us to further optimize the conditions using (*S*,*Rp*)-JosiPhos-3 as the ligand. In the screening of nickel(II) precursors, changing the $Ni(OAc)_2 \cdot 4H_2O$ to nickel salts of strong acids, $Ni(ClO_4)_2 \cdot 6H_2O$ and $Ni(OTf)_2$, the conversions were increased to 74% and 80%, respectively (entries 7 and 8, 97% ees). We were delighted to find that by employing $Ni(OTf)_2$ and switching the solvent from TFE to HFIP (hexafluoroisopropanol), the conversion increased to 89% with excellent enantioselectivity (99% ee, entries 9 vs 8). This is likely due to the increased positive charge on the Ni atom, which enhances its coordination ability with the polar groups in the substrate, leading to higher reactivity in the hydrogenation (conversions changed from 27 to 74/80%, from acetate to perchlorate/triflate). Increasing the solvent polarity has a similar effect (conversions changed from 80% in TFE to 89% in more polar HFIP).[16] Subsequently, the substrate can be converted completely when the ratio of nickel salt to ligand

https://doi.org/10.1021/jacs.4c10623
J. Am. Chem. Soc. XXXX, XXX, XXX−XXX

Scheme 2. Substrate Scope[a]

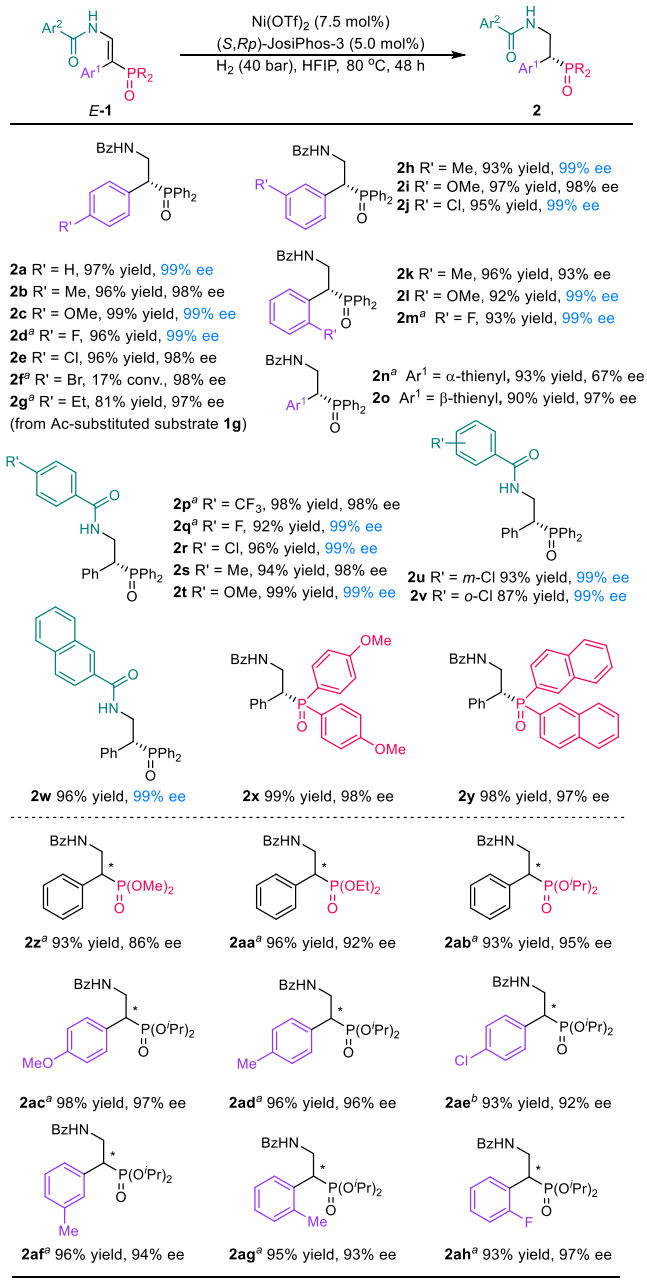

[a]Conditions: **1** (0.15 mmol), $Ni(OTf)_2$ (7.5 mol %), (*S,Rp*)-JosiPhos-3 (5.0 mol %), H_2 (40 bar), HFIP (2.5 mL), 80 °C, 48 h. [a]$Ni(OTf)_2$ (15 mol %), (*S,Rp*)-JosiPhos-3 (10 mol %). [b]$Ni(OTf)_2$ (22.5 mol %), (*S,Rp*)-JosiPhos-3 (15 mol %).

(M/L) is 1.5/1 (entries 10 vs 9). Other condition optimizations, including ligands, solvents, H_2 pressure, and the M/L ratio, did not improve the reaction (Tables S1 and S2). Therefore, the use of (*S,Rp*)-JosiPhos-3 (5.0 mol %) as the ligand and $Ni(OTf)_2$ (7.5 mol %) as the nickel source under 40 bar H_2 in HFIP at 80 °C for 24 h was selected as the standard reaction conditions. The absolute configuration of product **2a** was assigned to be *R* by X-ray crystallographic analysis (CCDC 2263840; see the Supporting Information for details).

During the initial substrate exploration, some substrates could not be fully transformed within 24 h. Therefore, a wide

Scheme 3. Ni-Catalyzed Asymmetric Hydrogenation of *Z*/*E* Isomeric Mixtures of *β*-Enamido Phosphine Oxides[a]

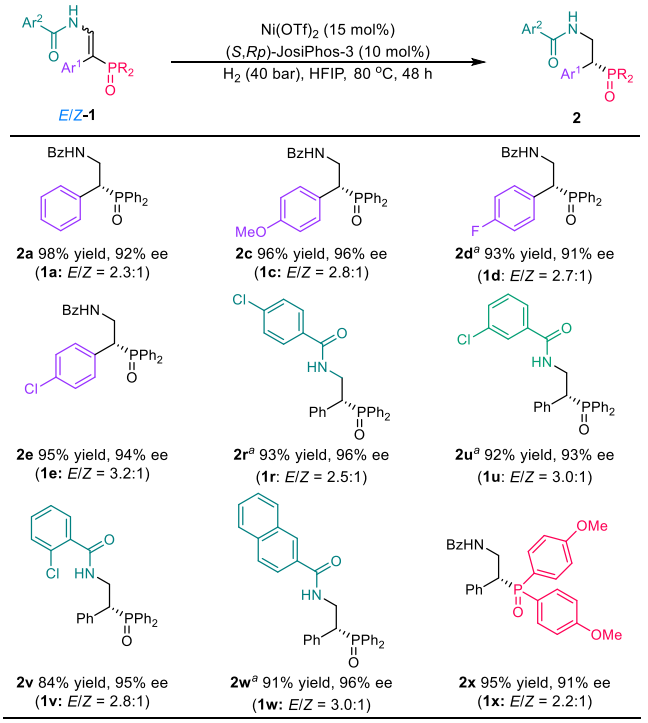

[a]Conditions: **1** (0.15 mmol), $Ni(OTf)_2$ (15 mol %), (*S,Rp*)-JosiPhos-3 (10 mol %), H_2 (40 bar), HFIP (2.5 mL), 80 °C, 48 h. [a] $Ni(OTf)_2$ (22.5 mol %), (*S,Rp*)-JosiPhos-3 (15 mol %).

scope of *E*-enamide phosphine oxides was tested with 48 h of reaction time (Scheme 2, top). At first, various *α*-aryl (Ar^1) substituted *E*-substrates (**1a**−**1o**) were submitted to hydrogenation, and most of them provided the corresponding products with excellent results (92−99% yields, with **2a**, **2c**, **2d**, **2h**, **2j**, **2l**, **2m**: 99% ees; **2b**, **2e**, **2i**: 98% ees; **2o**: 97% ee; **2k**: 93% ee), with **1d** (*p*-F) and **1m** (*o*-F) substrates requiring high catalyst loading (10 mol %) to ensure excellent yields. However, under standard hydrogenation conditions using 10% Ni catalyst, substrates **1f** (*p*-Br), **1g** (*p*-Ac), and **1n** (*α*-thienyl) gave the corresponding products with moderate to good results (**2f**: 17% conversion and 98% ee; an interesting deoxidized product **2g**: 81% yield and 97% ee; **2n**: 93% yield and 67% ee, respectively). Other functional group substrates (*p*-I, *p*-CN in Ar^1 and tetrasubstituted alkenes) were also tried but with poor results, as detailed in Scheme S1. Subsequently, substrates with different benzoyl groups (Ar^2) were also investigated (**1p**−**1v**). Besides the *p*-CF_3 (**1p**) and *p*-Me (**1s**) substrates only giving 98% ees (**2p** and **2s**), all other substrates (**1q**−**1r**, **1t**−**1v**) bearing different substituents at the *p*-, *m*-, or *o*-positions of the benzoyl group could furnish the hydrogenation products with 99% ee. Furthermore, 99% ee of the corresponding product (**2w**) was achieved using the substrate when Ar^2 was a *β*-naphthyl group (**1w**). Then, substrates with different R groups were also explored. When R changed to *p*-OMe-C_6H_4 (**1x**) and a *β*-naphthyl group (**1y**), the corresponding products were obtained with 98 and 97% ees, respectively.

After the exploration of the *E*-*β*-enamido phosphine oxides, we turned our attention to the asymmetric hydrogenation of *E*-enamido phosphonates (Scheme 2, bottom), which required increasing the catalyst loading to 10 mol % for full conversions

https://doi.org/10.1021/jacs.4c10623
J. Am. Chem. Soc. XXXX, XXX, XXX−XXX

Scheme 4. Gram-Scale Synthesis of 2a and the Synthetic Applications[a]

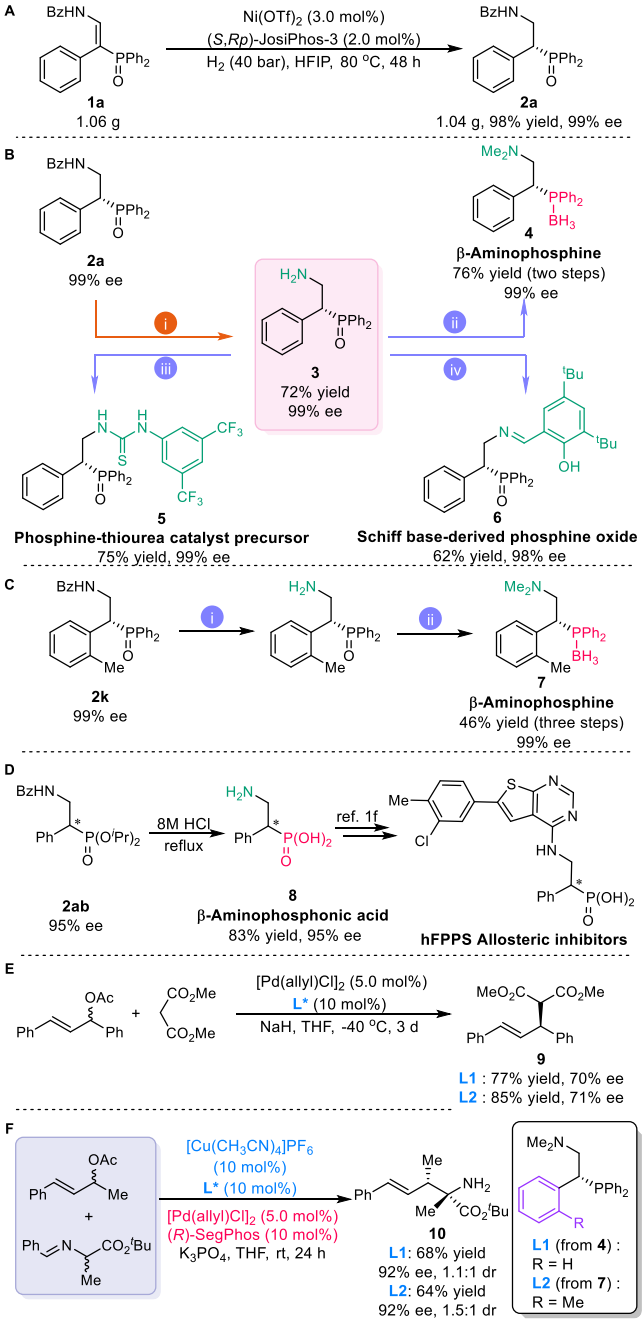

[a]Reaction conditions: (i) aq. HCl:1,4-dioxane (v:v) = 1:1, 120 °C. (ii) 1, HCOOH, HCHO, reflux; 2, $HSi(OEt)_3$, $Ti(O^iPr)_4$, toluene, 120 °C, then BH_3/THF, rt. (iii) 3,5-Bistrifluoromethylphenyl isothiocyanate, DCM, rt. (iv) 3,5-Di-*tert*-butylsalicylaldehyde, EtOH, reflux.

(93−98% yields). Methyl, ethyl, and isopropyl phosphonates (**1z**−**1ab**) were tolerated, providing the desired products with 86, 92, and 95% ees, respectively. Next, different α-phenyl substituted *E*-enamide isopropylphosphates (**1ac**−**1ah**) were explored, and all desired products exhibited good enantioselectivities (92−97% ees), although **1ae** required increasing the catalyst to 15 mol %.

In order to avoid the wastage of substrates and the hassle of separating β-enamido phosphine oxide isomers with different configurations, the compatibility of the Ni-catalytic system was investigated by using the synthesized *E*/*Z* isomeric mixtures (Scheme 3). Due to the relatively low activities of the *Z*-substrates, the catalyst loading was increased to 10 mol % to achieve full conversion. First, *Z*-**1a** was tested in this system to offer **2a** with 74% ee over 48 h. To our delight, the product from *Z*-**1a** has the same absolute configuration compared with *E*-**1a**. This implies that hydrogenation of substrates with different configurations could give the same enantiomer product.[7] The synthesized *E*/*Z*-**1a** mixture (*E*/*Z* = 2.3:1) was then hydrogenated, resulting in product **2a** with 92% ee. Next, several substrates bearing different Ar^1 (**1c**−**1e**) with different *E*/*Z* ratios were tested, and the desired products (**2c**−**2e**) were obtained in 91−96% ees. Subsequently, substrates with different Ar^2 (*p*-, *m*-, *o*-chloro phenyl (**1r**, **1u**, **1v**) and β-naphthyl group (**1w**)) were examined, yielding 93−96% ees. When R was changed to *p*-OMe-C_6H_4 (**1x**), the product **2x** was obtained with 91% ee. Among them, *p*-F-Ar^1 (**1d**), *p*-Cl-Ar^2 (**1r**), and *m*-Cl-Ar^2 (**1u**) substituted substrates and the substrate (**1w**) with an β-naphthyl group require 15 mol % catalyst for full conversion. These results indicate that the *E*/*Z* isomeric mixture of β-enamido phosphine oxides can also perform well in this Ni/JosiPhos catalytic system.

To demonstrate the potential synthetic application of this method (Scheme 4), a gram-scale experiment was performed with *E*-**1a**. The hydrogenation proceeded smoothly and gave **2a** in 98% yield with 99% ee using 2.0 mol % Ni catalyst (Scheme 4A). The benzoyl group in **2a** could be removed in a mixture of aq. HCl/dioxane to afford β-aminophosphine oxide **3**, which can undergo methylation, reduction, and borane protection to give β-aminophosphine **4** without any loss of enantioselectivity (Scheme 4B). β-Aminophosphine oxide **3** could also be used to synthesize the phosphine-thiourea catalyst precursor **5** and the Schiff base-derived phosphine oxide **6** in good results (Scheme 4B, **5**: 75% yield and 99% ee, **6**: 62% yield and 98% ee). As a precursor of the ligand, β-aminophosphine **7** could also be obtained from **2k** with 99% ee (Scheme 4C). β-Amido phosphonate **2ab** was easily converted into β-aminophosphonic acid **8** using 8 M HCl in 83% yield and 95% ee, which can be further transformed to hFPPS allosteric inhibitors (Scheme 4D).[1f] As distinctive P,N ligands, chiral β^2-amino phosphines have been underutilized in asymmetric catalytic reactions due to their challenging synthesis. Therefore, a Pd-catalyzed enantioselective alkylation reaction of allyl acetate was investigated using the novel chiral β^2-amino phosphine ligands **L1** and **L2**, which were obtained by in situ removal of the borane protection group from **4** and **7**, respectively (Scheme 4E). The desired product **9** was obtained in 77% yield, 70% ee and 85% yield, 71% ee using **L1** and **L2**, respectively. Subsequently, **L1** and **L2** were used in our previously reported challenging Pd/Cu catalysis for the dynamic kinetic asymmetric transformation of racemic unsymmetrical 1,3-disubstituted allyl acetates. The reaction gave the desired product **10** in 68% yield, 92% ee, 1.1:1 dr and 64% yield, 92% ee, 1.5:1 dr by using **L1** and **L2**, respectively (Scheme 4F). These reactions demonstrate the catalytic potential of β^2-aminophosphine as a ligand.

Mechanistic Studies. In general, two strategies have been used to achieve the same enantiomer of product from both *E*- and *Z*-alkene substrates in catalytic hydrogenation.[7] The most common method involves the rapid isomerization of the *E*- and *Z*-isomers, leading to dynamic kinetic resolution. Another less-common approach is to investigate a suitable catalytic

https://doi.org/10.1021/jacs.4c10623
J. Am. Chem. Soc. XXXX, XXX, XXX−XXX

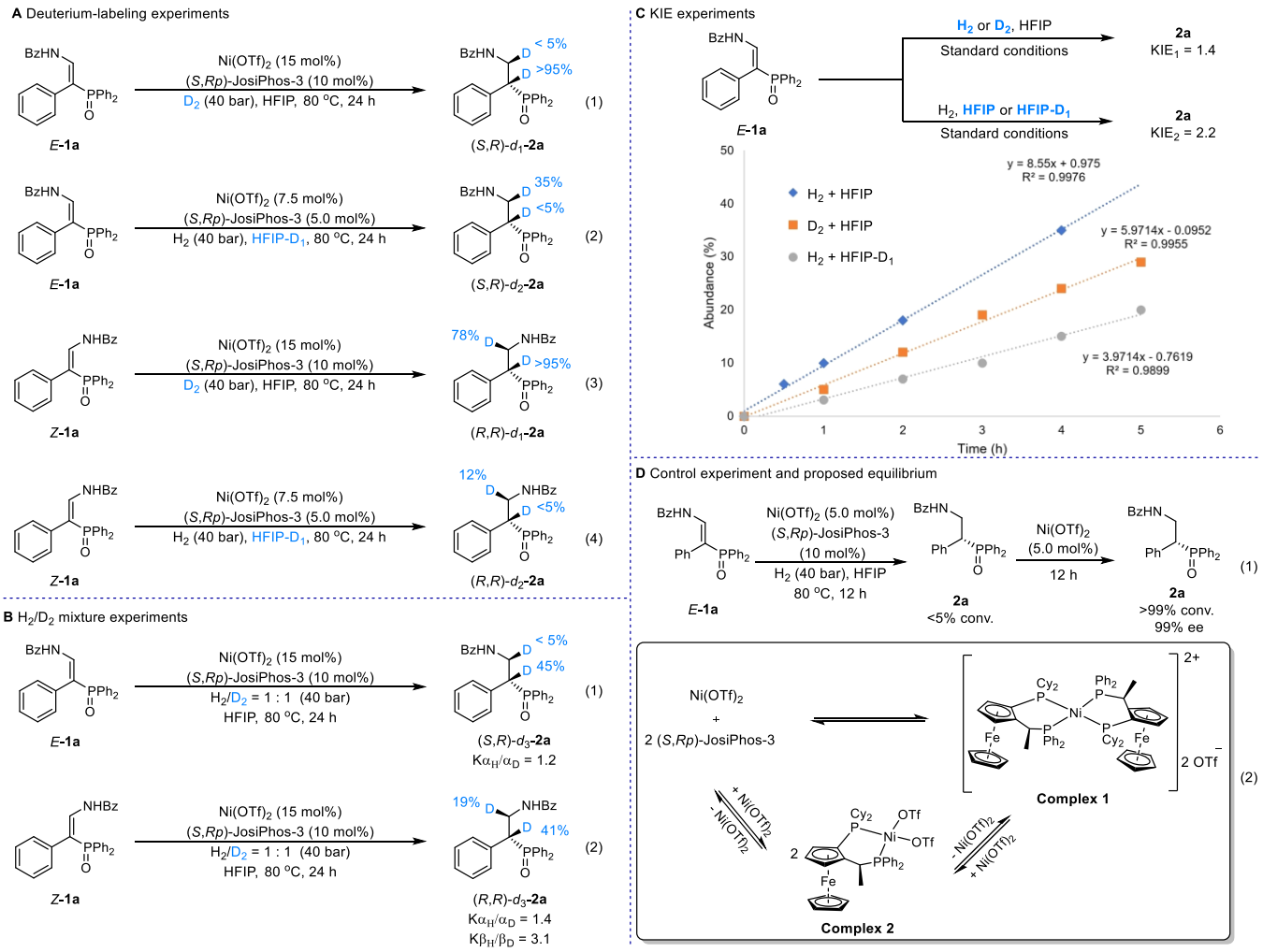

Figure 1. Control experiments. (A) Deuterium-labeling experiments. (B) H_2/D_2 mixture experiments. (C) KIE experiments. (D) Control experiment and proposed equilibrium.

Scheme 5. Proposed Mechanism

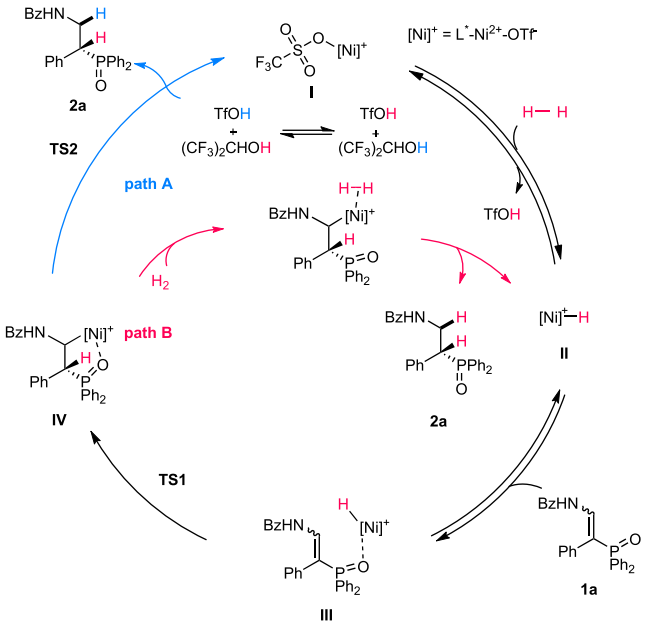

system capable of producing the same enantiomer product from both *E*- and *Z*-isomers. To validate this type of catalytic hydrogenation process in this Ni-catalytic system, the reaction was monitored, and almost no isomerization was observed for either the *E*- or *Z*-**1a** substrates under the standard reaction conditions (Figure S1). Next, a series of deuterium-labeling experiments were conducted (Figure 1A). Hydrogenation of *E*-**1a** under 40 bar D_2 in HFIP gave the product with full deuterium incorporation (>95%) at the α-position of the phosphine oxide group (Figure 1A, eq 1). When the reaction was carried out with H_2 and HFIP-D_1, the β-position of the phosphine oxide group was deuterated partially (35%, Figure 1A, eq 2). Switching the substrate to *Z*-**1a**, employing D_2 and conventional HFIP resulted in full deuterium incorporation (>95%) at the α-position and partial deuteration at the β-position (78%, Figure 1A, eq 3). Conversely, when the experiment was conducted under a H_2 atmosphere in HFIP-D_1, partial deuterium incorporation was observed at the β-position (12%, Figure 1A, eq 4). According to deuteration experiments (Figure 1A), it can be seen that the α-H of all products originates from H_2. However, the β-H of (*S*,*R*)-d_1-**2a** originates from the solvent (>95% H, Figure 1A, eq 1) and the β-D of (*R*,*R*)-d_1-**2a** mainly originates from D_2 (78% D, Figure 1A, eq 3). Therefore, when HFIP-D_1 and H_2 (Figure 1A, eq 2 and eq 4) were used, D incorporation at the β-position to the

https://doi.org/10.1021/jacs.4c10623
J. Am. Chem. Soc. XXXX, XXX, XXX−XXX

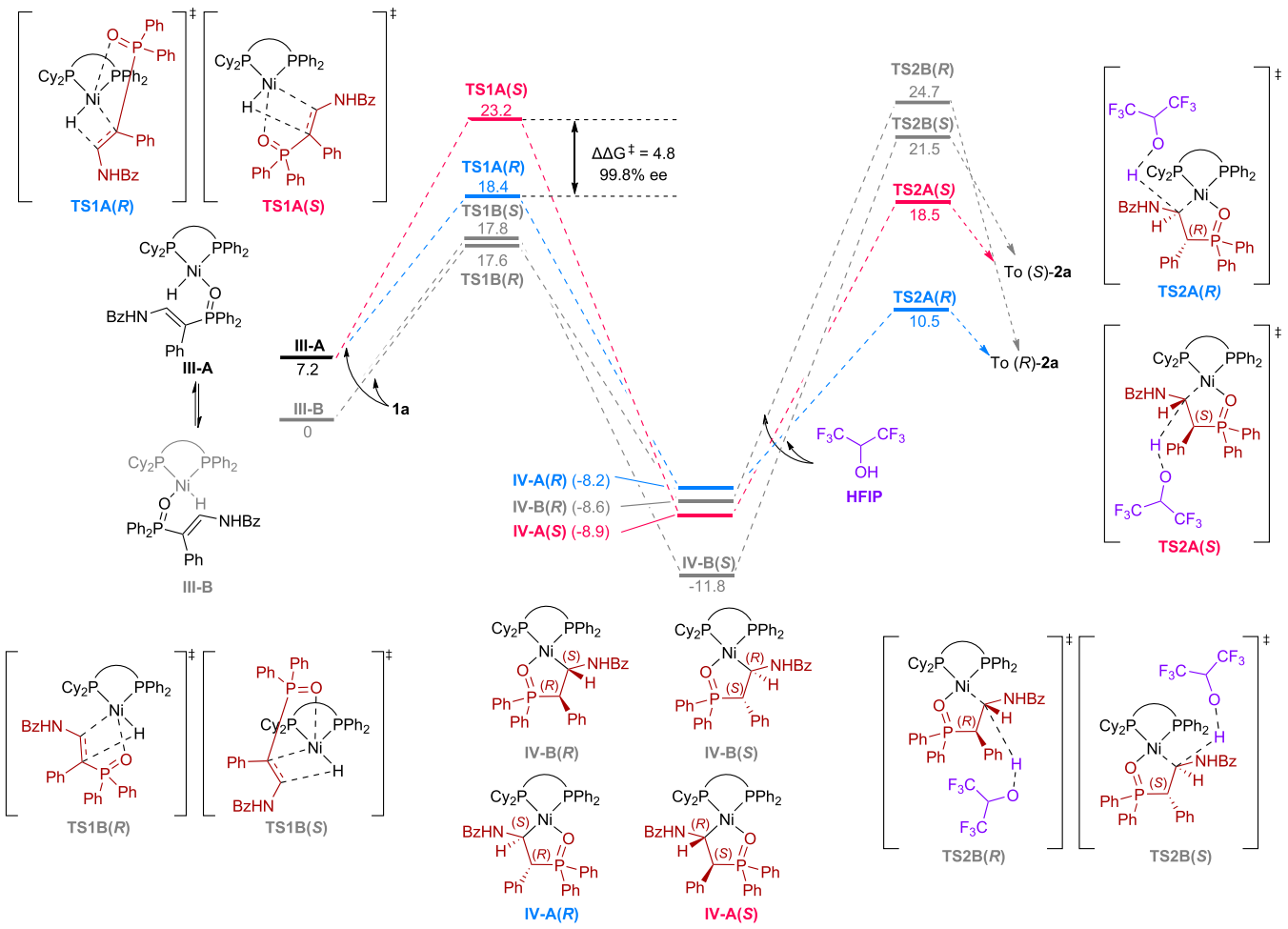

Figure 2. Computed Gibbs free energy profiles for the asymmetric hydrogenation of **1a** catalyzed by the Ni complex of (*S*,*Rp*)-JosiPhos-3. The free energies are obtained by adding the free energy corrections obtained in the ωB97XD/6-31G(d,p)/SMD(2,2,2-trifluoroethanol) optimizations to the single point energies computed at the ωB97XD/6-311G++(d,p)/SMD(2,2,2-trifluoroethanol) level of theory, 298.15 K, 1 bar.

phosphine oxide enhanced in (*S*,*R*)-d_2-2a (35% D, Figure 1A, eq 2) compared to (*R*,*R*)-d_2-2a (12% D, Figure 1A, eq 4). The decrease of *β*-D in (*S*,*R*)-d_2-**2a** and (*R*,*R*)-d_2-**2a** may be due to the higher activity of H^+ compared to D^+, which is produced by heterolysis of H_2 in the D-solvent (35% vs >95%, Figure 1A, eq 2 vs eq 1; 12% vs 22%, Figure 1A, eqs 4 vs 3). The formation of different diastereoisomers, (*S*,*R*)-d_1-**2a**, (*S*,*R*)-d_2-**2a**, (*R*,*R*)-d_1-**2a**, and (*R*,*R*)-d_2-**2a**, further suggests an absence of isomerization for both *E*- and *Z* -isomers.

To verify the rate-determining step of the reaction, hydrogenation of *E*- or *Z*-**1a** with a H_2/D_2 mixture and KIE experiments were conducted (Figure 1B,C). The H_2/D_2 mixture result of *E*-**1a** shows that the rate-determining step of the reaction is independent of hydrogen (Figure 1B, eq 1, $K\alpha_H/\alpha_D$ = 1.2). However, the reaction of *Z*-**1a** suggests that the addition of hydrogen atoms from H_2 to the *β*-position is the rate-determining step (Figure 1B, eq 2, $K\beta_H/\beta_D$ = 3.1). Next, according to Figure 1C, it was found that different KIEs of *E*-**1a** were observed when using H_2/D_2 in HFIP (KIE_1 = 1.4) and H_2 in HFIP/HFIP-D_1 (KIE_2 = 2.2). The results indicate that the protonation step with solvent participation should be the rate-determining step.

In the control experiments, no desired product was detected when 5.0 mol % $Ni(OTf)_2$ and 10 mol % (*S*,*Rp*)-JosiPhos-3 were used for the reaction. However, an additional 5.0 mol % $Ni(OTf)_2$ was added to the catalytic system, resulting in the complete conversion of **1a** (Figure 1D, eq 1). This result demonstrates that inactive Complex **1** (M/L = 1/2) is likely generated at first, and Complex **1** can be reactivated to generate Complex **2** (M/L = 1/1) when additional nickel salt is added (Figure 1D, eq 2). The coordination behavior of (*S*,*Rp*)-JosiPhos-3 with $Ni(OTf)_2$ in $(CF_3)_2CDOD$ with various ratios was then studied and analyzed using ^1H and ^{31}P NMR spectroscopies, along with HRMS analysis, to confirm the presence of the aforementioned complex structures (Figures S2−S5). We also detected the possible signal of the $[Ni]^+$−H complex in HRMS analysis when M/L was 1/1 (Figure S4).

Based on the above mechanistic experiment results (Figure 1), two possible catalytic cycles, path a and path b, are proposed in Scheme 5. The catalyst is monohydride cationic Ni(II) complex **II** ($[Ni]^+$−H), which forms during the initial stages of the reaction through the interaction of nickel complex **I** ($[Ni]^+$−OTf) with high-pressure hydrogen. The polar group of the substrate (P=O or C=O) coordinated to complex **II** to produce **III**, and subsequently, the double bond approaches the Ni atom and then migratory insertion occurs to form the chiral complex **IV**. Delivery of the second hydrogen atom can proceed via two different pathways. Thus, one could consider

https://doi.org/10.1021/jacs.4c10623
J. Am. Chem. Soc. XXXX, XXX, XXX−XXX

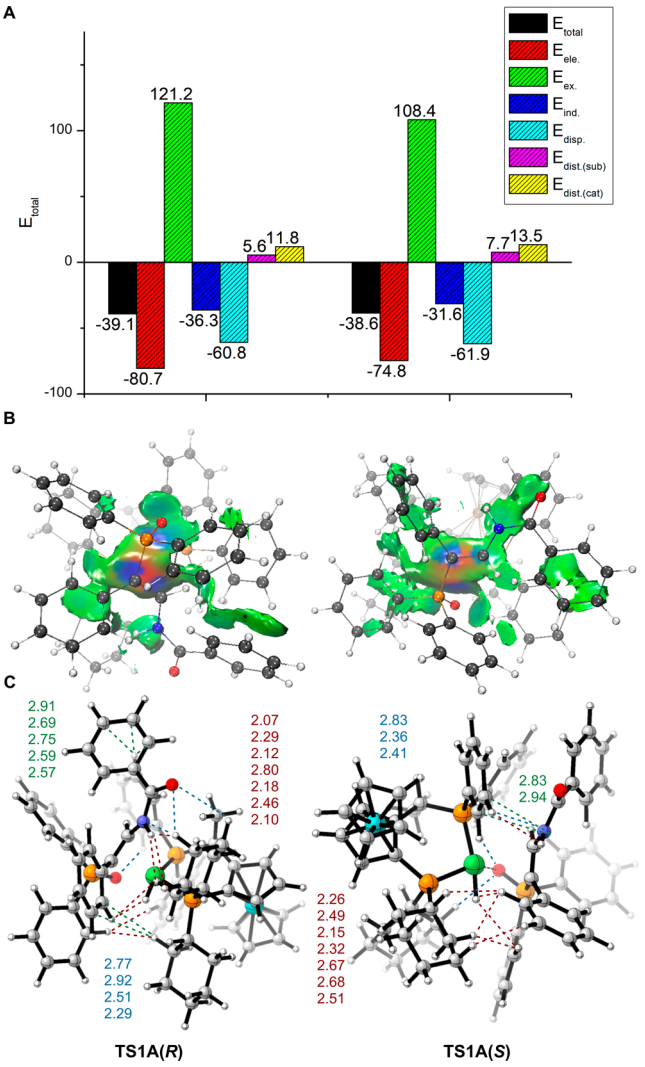

Figure 3. (A) Energy decomposition analysis (EDA). left: **TS1A**(***R***), right: **TS1A**(***S***). (B) Independent gradient model based on Hirshfeld partition (IGMH) analysis. (C) Optimized structures of **TS1A**(***R***) and **TS1A**(***S***). The weak attractive interactions (length in Å) in the range of 1.9−3.0 Å: red, CH···HX (X = C, N, Ni); blue, CH···Y (Y = O or N); green, CH···π.

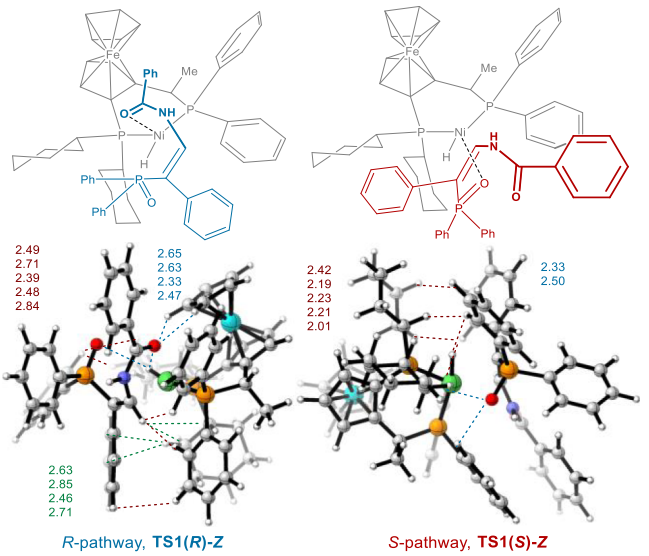

Figure 4. Possible modes of coordination of the *Z*-**1a** transition states. The weak attractive interactions (length in Å) in the range 1.9−3.0 Å are as follows: red, CH···HX (X = C, N, Ni); blue, XH···Y (X = C or Ni, Y = O or N); green, CH···π.

hydrogen metathesis, either assisted by the protonic solvent/acid (H^+) (path a)[14b,g] or H_2 (path b).[14b,c,e,f]

To investigate the mechanism of hydrogenation of *E*-**1a**, DFT calculations were also conducted. Considering the non-C_2-symmetric ligand, four major possible reaction pathways are conceivable (Figure 2). In the beginning, two kinds of intermediates of Ni−H with a substrate (**III-A** and **III-B**) can be formed. It is worth noting that the formation of Ni−H complex **II** and the coordination step are reversible; therefore, these two intermediates (**III-A** and **III-B**) can be easily interconverted. Then, during the approach toward Ni, the double bond of *E*-**1a** is inserted by the hydrogen atom simultaneously via **TS1**. A similar phenomenon was observed in previous studies, especially in substrates with large steric hindrance.[14a,c,e] After **TS1**, chelated intermediates **IV** with a five-membered ring are generated, and this whole coordination/migratory insertion step is exergonic. In the next step, the protonation of the C−Ni bond occurs with a molecule of HFIP via **TS2**, leading to the formation of the corresponding products.

Next, the energies in the Gibbs free energy profile were focused on. Since the first step is exergonic, the activation energy of the second step was calculated from the difference between **TS2** and **IV**. Hence, for the first step, the activation energies are 17.6−23.2 kcal/mol, while for the second step, the activation energies are 18.7−33.3 kcal/mol. These results suggest that the protonation step should be the rate-determining step, consistent with the KIE experiment (Figure 1C). However, when considering the stereo-determining step, the situation becomes more complex. In the gray pathways starting from **III-B**, the energies of **TS2B**(***R***) (24.7 kcal/mol) and **TS2B**(***S***) (21.5 kcal/mol) are significantly higher than those of **TS1B**(***R***) (17.6 kcal/mol) and **TS1B**(***S***) (17.8 kcal/mol), respectively. This suggests the reaction may stop at **IV-B**(***R***) and **IV-B**(***S***), and the first step should be reversible because of the lower activation energies of the reverse reaction (26.1 and 29.6 kcal/mol) compared to the subsequent one (both are 33.3 kcal/mol). On the contrary, for the colored (red and blue) pathways, the first step should be irreversible because of the higher activation energies of the reverse reaction (26.5 and 32.1 kcal/mol) compared to the subsequent one (18.7 and 27.4 kcal/mol). In this case, the colored pathway should be the major pathway, and the first step should be the stereo-determining step due to its irreversibility. As a result, the calculated major configuration of the product is *R* and the calculated ee based on the energy difference between **TS1A**(***R***) and **TS1A**(***S***) ($\Delta\Delta G^{\ddagger}$ = 4.8 kcal/mol) is 99.8%, which matches the experimental data (99% ee, Table 1, entry 10).

EDA was then employed to quantitatively measure the strength of the interactions between the substrate and the Ni catalyst (Figure 3A). It was found that the electrostatic energy, induction energy, and distortion energies in **TS1A**(***R***) are lower than those in **TS1A**(***S***). However, the exchange-repulsion energy is higher than that in **TS1A**(***S***). In total, **TS1A**(***R***) has a lower interaction energy compared to **TS1A**(***S***), which is consistent with the experimental configuration. The lower distortion energy suggests that the skeleton

https://doi.org/10.1021/jacs.4c10623
J. Am. Chem. Soc. XXXX, XXX, XXX−XXX

of the ligand enhances the enantioselectivity of the reaction. Additionally, other energy items suggest that the secondary interactions between the substrate and the Ni catalyst enhance the enantioselectivity of the reaction as well. The following IGMH analysis clearly exhibited these secondary interactions (Figure 3B), which are marked in the schematic diagram below. It can be observed that there are more CH···π and CH···O/N interactions in **TS1A(*R*)** than those in **TS1A(*S*)** (green and blue dashed lines in Figure 3C). These analyses demonstrated how the secondary interactions between the substrate and the Ni catalyst contribute to the enantioselectivity of the reaction.

Although in most cases, the resulting enantioselectivities are high enough (>90% ee) with *E*/*Z*-isomer mixtures, the enantioselectivity of the reaction is relatively low when using the *Z*-substrate (74% ee for **2a** from *Z*-**1a**). This level of enantioselectivity increases the difficulty of calculating the accuracy. In addition, the catalytic cycle of the *Z*-substrate may proceed through two pathways using solvent and H_2 dissociation, respectively (path A and path B, Figure 1A and Scheme 5). Thus, DFT calculations were conducted on the key transition states **TS1-*Z*** of *Z*-**1a** based on the *E*-**1a** catalytic cycle mentioned above (Figure 2). These calculations showed a significant preference for **TS1(*R*)-*Z*** over **TS1(*S*)-*Z***, which is consistent with the *R*-products observed in the experiments. Interestingly, computations showed that in the transition state of hydride transfer, the carbonyl group is coordinated to nickel instead of the P=O group as observed in the transition states for the hydrogenation of *E*-substrates. This kind of coordination leads to a cascade of CH···O, NiH···O, and CH···π weak attractive interactions (blue and green dashed lines in Figure 4), which enhance the stability of **TS1(*R*)-*Z***. In contrast, **TS1(*S*)-*Z*** lacks most of these interactions (Figure 4).

CONCLUSIONS

In conclusion, a novel method for the synthesis of chiral β^2-amino phosphorus derivatives has been achieved using an earth-abundant metal nickel catalyst in asymmetric hydrogenation. *E*-β-enamido phosphorus substrates exhibit perfect enantioselectivities, with most products (13 examples) achieving up to 99% ee. Even *E*/*Z*-substrate mixtures also yield good enantioselectivities (91−96% ees). These products can be further transformed to various valuable bioactive molecules, chiral organic catalysts, and chiral ligands. The possible reaction mechanism is elucidated through experiments and DFT calculations along with IGMH and EDA analyses. These findings suggest that the stable weak attractive interactions between the Ni catalyst and the substrate in the transition states are crucial for achieving excellent enantioselectivities. The DFT calculations also show that the formation of the same enantiomer product from the asymmetric hydrogenation of the *E*- or *Z*-substrate may arise due to their different coordination modes with the catalyst.

ASSOCIATED CONTENT

Supporting Information

The Supporting Information is available free of charge at https://pubs.acs.org/doi/10.1021/jacs.4c10623.

Experimental procedures, computational details, and characterization data for all reactions and products, including ^{1}H and ^{13}C NMR spectra, ^{19}F NMR spectra, ^{31}P NMR spectra, HPLC spectra, and crystallographic data for **2a** (CCDC 2263840) (PDF)

Accession Codes

Deposition Number 2263840 contains the supplementary crystallographic data for this paper. These data can be obtained free of charge via the joint Cambridge Crystallographic Data Centre (CCDC) and Fachinformationszentrum Karlsruhe Access Structures service.

AUTHOR INFORMATION

Corresponding Authors

Jianzhong Chen − *Shanghai Key Laboratory for Molecular Engineering of Chiral Drugs, Frontiers Science Center for Transformative Molecules, School of Chemistry and Chemical Engineering, Shanghai Jiao Tong University, Shanghai 200240, China*; Email: 0091109001@sjtu.edu.cn

Ilya D. Gridnev − *N.D. Zelinsky Institute of Organic Chemistry, Russian Academy of Sciences, Moscow 119991, Russian Federation*; Email: ilyaiochem@gmail.com

Wanbin Zhang − *Shanghai Key Laboratory for Molecular Engineering of Chiral Drugs, Frontiers Science Center for Transformative Molecules, School of Chemistry and Chemical Engineering, Shanghai Jiao Tong University, Shanghai 200240, China*; orcid.org/0000-0002-4788-4195; Email: wanbin@sjtu.edu.cn

Authors

Hanlin Wei − *Shanghai Key Laboratory for Molecular Engineering of Chiral Drugs, Frontiers Science Center for Transformative Molecules, School of Chemistry and Chemical Engineering, Shanghai Jiao Tong University, Shanghai 200240, China*

Yicong Luo − *Shanghai Key Laboratory for Molecular Engineering of Chiral Drugs, Frontiers Science Center for Transformative Molecules, School of Chemistry and Chemical Engineering, Shanghai Jiao Tong University, Shanghai 200240, China*

Jinhui Li − *Shanghai Key Laboratory for Molecular Engineering of Chiral Drugs, Frontiers Science Center for Transformative Molecules, School of Chemistry and Chemical Engineering, Shanghai Jiao Tong University, Shanghai 200240, China*

Complete contact information is available at: https://pubs.acs.org/10.1021/jacs.4c10623

Notes

The authors declare no competing financial interest.

ACKNOWLEDGMENTS

This work was financially supported by the National Key R&D Program of China (No. 2023YFA1506400), the National Natural Science Foundation of China (Nos. 22361132533, 21991112, and 22471157), the Russian Science Foundation (No. 24-43-00011), and the Postdoctoral Fellowship Program of CPSF (No. GZC20240994). The authors thank the Instrumental Analysis Center of SJTU for characterization.

REFERENCES

(1) (a) Schoepp, D. D.; Johnson, B. G. Inhibition of Excitatory Amino Acid-Stimulated Phosphoinositide Hydrolysis in the Neonatal Rat Hippocampus by 2-Amino-3-Phosphonopropionate. *J. Neurochem.* **1989**, *53*, 1865−1870. (b) Balzarini, J.; Holy, A.; Jindrich, J.; Naesens,

L.; Snoeck, R.; Schols, D.; De Clercq, E. Differential Antiherpesvirus and Antiretrovirus Effects of the (*S*) and (*R*) Enantiomers of Acyclic Nucleoside Phosphonates: Potent and Selective in Vitro and in Vivo Antiretrovirus Activities of (*R*)-9-(2-Phosphonomethoxypropyl)-2,6-diaminopurine. *Antimicrob. Agents Chemother.* **1993**, *37*, 332−338. (c) Yokomatsu, T.; Sato, M.; Shibuya, S. Lipase-Catalyzed Enantioselective Acylation of Prochiral 2-(ω-Phosphono)alkyl-13-propane diols Application to the Enantioselective Synthesis of ω-Phosphono-α-amino Acids. *Tetrahedron Asymmetry* **1996**, *7*, 2743−2754. (d) Herczegh, P.; Buxton, T. B.; McPherson, J. C.; Kovács-Kulyassa, Á.; Brewer, P. D.; Sztaricskai, F.; Stroebel, G. G.; Plowman, K. M.; Farcasiu, D.; Hartmann, J. F. Osteoadsorptive Bisphosphonate Derivatives of Fluoroquinolone Antibacterials. *J. Med. Chem.* **2002**, *45*, 2338−2341. (e) Albrecht, S.; Defoin, A.; Salomon, E.; Tarnus, C.; Wetterholm, A.; Haeggström, J. Z. Synthesis and Structure Activity Relationships of Novel Non-Peptidic Metallo-Aminopeptidase Inhibitors. *Bioorg. Med. Chem.* **2006**, *14*, 7241−7257. (f) Park, J.; Leung, C. Y.; Matralis, A. N.; Lacbay, C. M.; Tsakos, M.; Fernandez De Troconiz, G.; Berghuis, A. M.; Tsantrizos, Y. S. Pharmacophore Mapping of Thienopyrimidine-Based Monophosphonate (ThP-MP) Inhibitors of the Human Farnesyl Pyrophosphate Synthase. *J. Med. Chem.* **2017**, *60*, 2119−2134.

(2) (a) Kafarski, P.; Lejczak, B. Biological Activity of Aminophosphonic Acids. *Phosphorus, Sulfur Silicon Relat. Elem.* **1991**, *63*, 193−215. (b) Hudson, H. R.; Kukhar, V. P. *Aminophosphonic and Aminophosphinic Acids: Chemistry and Biological Activity*; Wiley: Chichester, 2000. (c) Palacios, F.; Alonso, C.; de los Santos, J. M. Synthesis of β-Aminophosphonates and -Phosphinates. *Chem. Rev.* **2005**, *105*, 899−932. (d) Demmer, C. S.; Krogsgaard-Larsen, N.; Bunch, L. Review on Modern Advances of Chemical Methods for the Introduction of a Phosphonic Acid Group. *Chem. Rev.* **2011**, *111*, 7981−8006.

(3) (a) Carroll, M. P.; Guiry, P. J. P,N Ligands in Asymmetric Catalysis. *Chem. Soc. Rev.* **2014**, *43*, 819−833. (b) Li, W.; Zhang, J. Recent Developments in the Synthesis and Utilization of Chiral β-Aminophosphine Derivatives as Catalysts or Ligands. *Chem. Soc. Rev.* **2016**, *45*, 1657−1677. (c) Zirakzadeh, A.; Kirchner, K.; Roller, A.; Stöger, B.; Widhalm, M.; Morris, R. H. Iron(II) Complexes Containing Chiral Unsymmetrical PNP′ Pincer Ligands: Synthesis and Application in Asymmetric Hydrogenations. *Organometallics* **2016**, *35*, 3781−3787.

(4) Selected papers: (a) Terada, M.; Ikehara, T.; Ube, H. Enantioselective 1,4-Addition Reactions of Diphenyl Phosphite to Nitroalkenes Catalyzed by an Axially Chiral Guanidine. *J. Am. Chem. Soc.* **2007**, *129*, 14112−14113. (b) Fu, X.; Jiang, Z.; Tan, C.-H. Bicyclic Guanidine-Catalyzed Enantioselective Phospha-Michael Reaction Synthesis of Chiral β-Aminophosphine Oxides and β-Aminophosphines. *Chem. Commun.* **2007**, 5058−5060. (c) Wang, J.; Heikkinen, L. D.; Li, H.; Zu, L.; Jiang, W.; Xie, H.; Wang, W. Quinine-Catalyzed Enantioselective Michael Addition of Diphenyl Phosphite to Nitroolefins: Synthesis of Chiral Precursors of α-Substituted β-Aminophosphonates. *Adv. Synth. Catal.* **2007**, *349*, 1052−1056. (d) Bartoli, G.; Bosco, M.; Carlone, A.; Locatelli, M.; Mazzanti, A.; Sambri, L.; Melchiorre, P. Organocatalytic Asymmetric Hydrophosphination of Nitroalkenes. *Chem. Commun.* **2007**, 722−724. (e) Feng, J.-J.; Huang, M.; Lin, Z.-Q.; Duan, W.-L. Palladium-Catalyzed Asymmetric 1,4-Addition of Diarylphosphines to Nitroalkenes for the Synthesis of Chiral P. *N*-Compounds. *Adv. Synth. Catal.* **2012**, *354*, 3122−3126. (f) Ding, B.; Zhang, Z.; Xu, Y.; Liu, Y.; Sugiya, M.; Imamoto, T.; Zhang, W. P-Stereogenic PCP Pincer-Pd Complexes: Synthesis and Application in Asymmetric Addition of Diarylphosphines to Nitroalkenes. *Org. Lett.* **2013**, *15*, 5476−5479.

(5) Selected reviews for transition metal-catalyzed asymmetric hydrogenation (a) Tang, W.; Zhang, X. New Chiral Phosphorous Ligands for Enantioselective Hydrogenation. *Chem. Rev.* **2003**, *103*, 3029−3070. (b) Chen, Q. A.; Ye, Z. S.; Duan, Y.; Zhou, Y. G. Homogeneous Palladium-Catalyzed Asymmetric Hydrogenation. *Chem. Soc. Rev.* **2013**, *42*, 497−511. (c) Verendel, J. J.; Pàmies, O.; Diéguez, M.; Andersson, P. G. Asymmetric Hydrogenation of Olefins Using Chiral Crabtree-type Catalysts: Scope and Limitations. *Chem. Rev.* **2014**, *114*, 2130−2169. (d) Zhang, Z.; Butt, N. A.; Zhang, W. Asymmetric Hydrogenation of Nonaromatic Cyclic Substrates. *Chem. Rev.* **2016**, *116*, 14769−14821. (e) Ponra, S.; Boudet, B.; Phansavath, P.; Ratovelomanana-Vidal, V. Recent Developments in Transition-Metal-Catalyzed Asymmetric Hydrogenation of Enamides. *Synthesis* **2021**, *53*, 193−214. (f) Yang, F.; Xie, J.-H.; Zhou, Q.-L. Highly Efficient Asymmetric Hydrogenation Catalyzed by Iridium Complexes with Tridentate Chiral Spiro Aminophosphine Ligands. *Acc. Chem. Res.* **2023**, *56*, 332−349. (g) Lückemeier, L.; Pierau, M.; Glorius, F. Asymmetric Arene Hydrogenation: Towards Sustainability and Application. *Chem. Soc. Rev.* **2023**, *52*, 4996−5012. (h) Yang, H.; Yu, H.; Stolarzewicz, I. A.; Tang, W. Enantioselective Transformations in the Synthesis of Therapeutic Agents. *Chem. Rev.* **2023**, *123*, 9397−9446. (i) Imamoto, T. P-Stereogenic Phosphorus Ligands in Asymmetric Catalysis. *Chem. Rev.* **2024**, *124*, 8657−8739. The latest representative articles: (j) Xu, Y.; Luo, Y.; Ye, J.; Liu, D.; Zhang, W. Rh-Catalyzed Enantioselective Desymmetric Hydrogenation of α-Acetamido-1,3-indanediones Using Ether-Bridged Biphenyl diphosphine Ligands. *J. Am. Chem. Soc.* **2023**, *145*, 21176−21182. (k) Li, K.; Wu, W.-Q.; Lin, Y.; Shi, H. Asymmetric hydrogenation of 1,1-diarylethylenes and benzophenones through a relay strategy. *Nat. Commun.* **2023**, *14*, 2170. (l) Xu, L.; Yang, T.; Sun, H.; Zeng, J.; Mu, S.; Zhang, X.; Chen, G.-Q. Rhodium-Catalyzed Asymmetric Hydrogenation and Transfer Hydrogenation of 1,3-Dipolar Nitrones. *Angew. Chem., Int. Ed.* **2024**, *63*, No. e202319662. (m) Wang, Z.; Yang, X.-Y.; Xu, Y.; Zhou, Q.-L. Iridium-Catalyzed Asymmetric Hydrogenation of Dialkyl Imines. *CCS Chem.* **2024**, *6*, 905−911. (n) Rong, N.; Zhou, A.; Liang, M.; Wang, S.-G.; Yin, Q. Asymmetric Hydrogenation of Racemic 2-Substituted Indoles via Dynamic Kinetic Resolution: An Easy Access to Chiral Indolines Bearing Vicinal Stereogenic Centers. *J. Am. Chem. Soc.* **2024**, *146*, 5081−5087.

(6) (a) Kadyrov, R.; Holz, J.; Schäffner, B.; Zayas, O.; Almena, J.; Börner, A. Synthesis of Chiral β-Aminophosphonates via Rh-Catalyzed Asymmetric Hydrogenation of β-Amido-Vinyl phosphonates. *Tetrahedron Asymmetry* **2008**, *19*, 1189−1192. (b) Doherty, S.; Knight, J. G.; Bell, A. L.; El-Menabawey, S.; Vogels, C. M.; Decken, A.; Westcott, S. A. Rhodium Complexes of (R)-Me-CATPHOS and (R)-(S)-JosiPhos Highly Enantioselective Catalysts for the Asymmetric Hydrogenation of (E)- and (Z)-β-aryl-β-(Enamido)-Phosphonates. *Tetrahedron Asymmetry* **2009**, *20*, 1437−1444. (c) Zhang, J.; Li, Y.; Wang, Z.; Ding, K. Asymmetric Hydrogenation of α- and β-Enamido Phosphonates: Rhodium(I)/Monodentate Phosphoramidite Catalyst. *Angew. Chem., Int. Ed.* **2011**, *50*, 11743−11747. (d) Chávez, M. Á.; Vargas, S.; Suárez, A.; Álvarez, E.; Pizzano, A. Highly Enantioselective Hydrogenation of β-Acyloxy and β-Acylamino α,β-Unsaturated Phosphonates Catalyzed by Rhodium Phosphane-Phosphite Complexes. *Adv. Synth. Catal.* **2011**, *353*, 2775−2794. (e) Du, H.-Q.; Hu, X.-P. Rh-Catalyzed Asymmetric Hydrogenation of (*Z*)-β-Phosphorylated Enamides: Highly Enantioselective Access to β-Aminophosphines. *Org. Lett.* **2019**, *21*, 8921−8924. (f) Zhang, J.-H.; Xu, H.; Tang, X.; Dang, Y.; Zhang, F.-G.; Ma, J.-A. Highly Enantio- and Diastereoselective Hydrogenation of Cyclic Tetra-Substituted β-Enamido Phosphorus Derivatives. *Angew. Chem., Int. Ed.* **2023**, *62*, No. e202305315. (g) Kondoh, A.; Yorimitsu, H.; Oshima, K. Regio- and Stereoselective Hydroamidation of 1-Alkynylphosphine Sulfides Catalyzed by Cesium Base. *Org. Lett.* **2008**, *10*, 3093−3095.

(7) (a) Gridnev, I. D.; Imamoto, T.; Hoge, G.; Kouchi, M.; Takahashi, H. Asymmetric Hydrogenation Catalyzed by a Rhodium Complex of (*R*)-(*tert*-Butylmethylphosphino)(di-*tert*-butylphosphino)-methane: Scope of Enantioselectivity and Mechanistic Study. *J. Am. Chem. Soc.* **2008**, *130*, 2560−2572. (b) Bernasconi, M.; Müller, M.-A.; Pfaltz, A. Asymmetric Hydrogenation of Maleic Acid Diesters and Anhydrides. *Angew. Chem., Int. Ed.* **2014**, *53*, 5385−5388. (c) Yang, J.; Massaro, L.; Krajangsri, S.; Singh, T.; Su, H.; Silvi, E.; Ponra, S.; Eriksson, L.; Ahlquist, M. S. G.; Andersson, P. G. Combined Theoretical and Experimental Studies Unravel Multiple Pathways to Convergent Asymmetric Hydrogenation of Enamides. *J.*

https://doi.org/10.1021/jacs.4c10623
J. Am. Chem. Soc. XXXX, XXX, XXX−XXX

Am. Chem. Soc. **2021**, *143*, 21594−21603. (d) Massaro, L.; Zheng, J.; Margarita, C.; Andersson, P. G. Enantioconvergent and Enantiodivergent Catalytic Hydrogenation of Isomeric Olefins. *Chem. Soc. Rev.* **2020**, *49*, 2504−2522. (e) Peters, B. B. C.; Zheng, J.; Birke, N.; Singh, T.; Andersson, P. G. Iridium-Catalyzed Enantioconvergent Hydrogenation of Trisubstituted Olefins. *Nat. Commun.* **2022**, *13*, 361. (f) Lu, P.; Wang, H.; Mao, Y.; Hong, X.; Lu, Z. Cobalt-Catalyzed Enantioconvergent Hydrogenation of Minimally Functionalized Isomeric Olefins. *J. Am. Chem. Soc.* **2022**, *144*, 17359−17364. (g) Chen, T.; Zou, Y.; Hu, Y.; Zhang, Z.; Wei, H.; Wei, L.; Zhang, W. Cobalt-Catalyzed Efficient Convergent Asymmetric Hydrogenationof *E*/*Z*-Enamides. *Angew. Chem., Int. Ed.* **2023**, *62*, No. e202303488.

(8) Reviews: (a) Chirik, P. J. Iron- and Cobalt-Catalyzed Alkene Hydrogenation: Catalysis with Both Redox-Active and Strong Field Ligands. *Acc. Chem. Res.* **2015**, *48*, 1687−1695. (b) Zhang, Z.; Butt, N. A.; Zhou, M.; Liu, D.; Zhang, W. Asymmetric Transfer and Pressure Hydrogenation with Earth-Abundant Transition Metal Catalysts. *Chin. J. Chem.* **2018**, *36*, 443−454. (c) Ai, W.; Zhong, R.; Liu, X.; Liu, Q. Hydride Transfer Reactions Catalyzed by Cobalt Complexes. *Chem. Rev.* **2019**, *119*, 2876−2953. (d) Wen, J.; Wang, F.; Zhang, X. Asymmetric Hydrogenation Catalyzed by First-row Transition Metal Complexes. *Chem. Soc. Rev.* **2021**, *50*, 3211−3237. (e) González-Sebastián, L.; Reyes-Sanchez, A.; Morales-Morales, D. Hydrogenation and Cross-Coupling Reactions Catalyzed by Mn, Fe, and Co Aromatic Pincer Complexes. *Organometallics* **2023**, *42*, 2426−2446. (f) Cai, X.; Chen, J.; Zhang, W. Development of Construction of Chiral C−X Bonds through Nickel Catalyzed Asymmetric Hydrogenation. *Acta Chim. Sinica* **2023**, *81*, 646−656. (g) Chakrabortty, S.; de Bruin, B.; de Vries, J. G. Cobalt-Catalyzed Asymmetric Hydrogenation: Substrate Specificity and Mechanistic Variability. *Angew. Chem., Int. Ed.* **2024**, *63*, No. e202315773.

(9) The latest representative articles: (a) Chakrabortty, S.; Konieczny, K.; de Zwart, F. J.; Bobylev, E. O.; Baráth, E.; Tin, S.; Müller, B. H.; Reek, J. N. H.; de Bruin, B.; de Vries, J. G. Cobalt-Catalyzed Enantioselective Hydrogenation of Trisubstituted Carbocyclic Olefins: An Access to Chiral Cyclic Amides. *Angew. Chem., Int. Ed.* **2023**, *62*, No. e202301329. (b) Oates, C. L.; Goodfellow, A. S.; Buhl, M.; Clarke, M. L. Rational Design of a Facially Coordinating P,N,N Ligand for Manganese-Catalysed Enantioselective Hydrogenation of Cyclic Ketones. *Angew. Chem., Int. Ed.* **2023**, *62*, No. e202212479. (c) Hu, Y.; Zou, Y.; Yang, H.; Ji, H.; Jin, Y.; Zhang, Z.; Liu, Y.; Zhang, W. Precise Synthesis of Chiral Z-Allylamides by Cobalt-Catalyzed Asymmetric Sequential Hydrogenations. *Angew. Chem., Int. Ed.* **2023**, *62*, No. e202217871. (d) Liu, C.; Liu, X.; Liu, Q. Stereodivergent Asymmetric Hydrogenation of Quinoxalines. *Chem.* **2023**, *9*, 2585−2600. (e) Guan, J.; Chen, J.; Luo, Y.; Guo, L.; Zhang, W. Copper-Catalyzed Chemoselective Asymmetric Hydrogenation of C = O Bonds of Exocyclic α,β-Unsaturated Pentanones. *Angew. Chem., Int. Ed.* **2023**, *62*, No. e202306380. (f) Wang, M.; Liu, S.; Liu, H.; Wang, Y.; Lan, Y.; Liu, Q. Asymmetric Hydrogenation of Ketimines with Minimally Different Alkyl Groups. *Nature* **2024**, *631*, 556−562.

(10) (a) Hamada, Y.; Koseki, Y.; Fujii, T.; Maeda, T.; Hibino, T.; Makino, K. Catalytic Asymmetric Hydrogenation of α-Amino-β-Keto Ester Hydrochlorides using Homogeneous Chiral Nickel-Bisphosphine Complexes through DKR. *Chem. Commun.* **2008**, *46*, 6206−6208. (b) Hibino, T.; Makino, K.; Sugiyama, T.; Hamada, Y. Homogeneous Chiral Nickel-Catalyzed Asymmetric Hydrogenation of Substituted Aromatic α-Aminoketone Hydrochlorides through Dynamic Kinetic Resolution. *ChemCatChem.* **2009**, *1*, 237−240.

(11) Selected papers for asymmetric transfer hydrogenation: (a) Yang, P.; Xu, H.; Zhou, J. Nickel-Catalyzed Asymmetric Transfer Hydrogenation of Olefins for the Synthesis of α- and β-Amino Acids. *Angew. Chem., Int. Ed.* **2014**, *53*, 12210−12213. (b) Yang, P.; Lim, L. H.; Chuanprasit, P.; Hirao, H.; Zhou, J. Nickel-Catalyzed Enantioselective Reductive Amination of Ketones with Both Arylamines and Benzhydrazide. *Angew. Chem., Int. Ed.* **2016**, *55*, 12083−12087. (c) Zhao, X.; Xu, H.; Huang, X.; Zhou, J. Asymmetric Stepwise Reductive Amination of Sulfonamides, Sulfamates, and a Phosphinamide by Nickel Catalysis. *Angew. Chem., Int. Ed.* **2019**, *58*, 292−296. (d) Yang, P.; Sun, Y.; Fu, K.; Zhang, L.; Yang, G.; Yue, J.; Ma, Y.; Zhou, J.; Tang, B. Enantioselective Synthesis of Chiral Carboxylic Acids from Alkynes and Formic Acid by Nickel-Catalyzed Cascade Reactions: Facile Synthesis of Profens. *Angew. Chem., Int. Ed.* **2022**, *61*, No. e202111778. (e) Li, A.; Song, X.; Ren, Q.; Bao, P.; Long, X.; Huang, F.; Yuan, L.; Zhou, J.; Qin, X. Cobalt-Catalyzed Asymmetric Deuteration of α-Amidoacrylates for Stereoselective Synthesis of α,β-Dideuterated α-Amino Acids. *Angew. Chem., Int. Ed.* **2023**, *62*, No. e202301091. (f) Sun, Y.; Wang, C.; Yang, P.; Yue, J.-Y.; Xu, C.; Zhou, J.; Tang, B. Hydrogen Bond Enhanced Enantioselectivity in the Nickel-Catalyzed Transfer Hydrogenation of α-Substituted Acrylic Acid with Formic Acid. *ACS Catal.* **2023**, *13*, 14213−14220.

(12) Shevlin, M.; Friedfeld, M. R.; Sheng, H.; Pierson, N. A.; Hoyt, J. M.; Campeau, L.-C.; Chirik, P. J. Nickel-Catalyzed Asymmetric Alkene Hydrogenation of α,β-Unsaturated Esters: High-Throughput Experimentation-Enabled Reaction Discovery, Optimization, and Mechanistic Elucidation. *J. Am. Chem. Soc.* **2016**, *138*, 3562−3569.

(13) Selected papers: (a) Gao, W.; Lv, H.; Zhang, T.; Yang, Y.; Chung, L. W.; Wu, Y.-D.; Zhang, X. Nickel-Catalyzed Asymmetric Hydrogenation of β-Acylamino Nitroolefins: an Efficient Approach to Chiral Amines. *Chem. Sci.* **2017**, *8*, 6419−6422. (b) Long, J.; Gao, W.; Guan, Y.; Lv, H.; Zhang, X. Nickel-Catalyzed Highly Enantioselective Hydrogenation of β-Acetylamino Vinylsulfones: Access to Chiral β-Amido Sulfones. *Org. Lett.* **2018**, *20*, 5914−5917. (c) Guan, Y.-Q.; Han, Z.; Li, X.; You, C.; Tan, X.; Lv, H.; Zhang, X. A Cheap Metal for a Challenging Task: Nickel-Catalyzed Highly Diastereo- and Enantioselective Hydrogenation of Tetrasubstituted Fluorinated Enamides. *Chem. Sci.* **2019**, *10*, 252−256. (d) You, C.; Li, X.; Gong, Q.; Wen, J.; Zhang, X. Nickel-Catalyzed Desymmetric Hydrogenation of Cyclohexadienones: An Efficient Approach to All-Carbon Quaternary Stereocenters. *J. Am. Chem. Soc.* **2019**, *141*, 14560−14564. (e) Liu, Y.; Yi, Z.; Yang, X.; Wang, H.; Yin, C.; Wang, M.; Dong, X.-Q.; Zhang, X. Efficient Access to Chiral 2-Oxazolidinones via Ni-Catalyzed Asymmetric Hydrogenation: Scope Study, Mechanistic Explanation, and Origin of Enantioselectivity. *ACS Catal.* **2020**, *10*, 11153−11161. (f) Liu, G.; Tian, K.; Li, C.; You, C.; Tan, X.; Zhang, H.; Zhang, X.; Dong, X.-Q. Nickel-Catalyzed Asymmetric Hydrogenation of Cyclic Alkenyl Sulfones, Benzo[*b*]-thiophene 1,1-Dioxides, with Mechanistic Studies. *Org. Lett.* **2021**, *23*, 668−675. (g) Liu, G.; Yang, X.; Gu, P.; Wang, M.; Zhang, X.; Dong, X.-Q. Challenging Task of Ni-Catalyzed Highly Regio-/Enantioselective Semihydrogenation of Racemic Tetrasubstituted Allenes via a Kinetic Resolution Process. *J. Am. Chem. Soc.* **2024**, *146*, 7419−7430.

(14) (a) Li, B.; Chen, J.; Zhang, Z.; Gridnev, I. D.; Zhang, W. Nickel-Catalyzed Asymmetric Hydrogenation of N-Sulfonyl Imines. *Angew. Chem., Int. Ed.* **2019**, *58*, 7329−7334. (b) Hu, Y.; Chen, J.; Li, B.; Zhang, Z.; Gridnev, I. D.; Zhang, W. Nickel-Catalyzed Asymmetric Hydrogenation of 2-Amidoacrylates. *Angew. Chem., Int. Ed.* **2020**, *59*, 5371−5375. (c) Liu, D.; Li, B.; Chen, J.; Gridnev, I. D.; Yan, D.; Zhang, W. Ni-Catalyzed Asymmetric Hydrogenation of N-Aryl Imino Esters for the Efficient Synthesis of Chiral α-Aryl Glycines. *Nat. Commun.* **2020**, *11*, 5935. (d) Li, B.; Liu, D.; Hu, Y.; Chen, J.; Zhang, Z.; Zhang, W. Nickel-Catalyzed Asymmetric Hydrogenation of Hydrazones. *Eur. J. Org. Chem.* **2021**, 3421−3425. (e) Li, B.; Chen, J.; Liu, D.; Gridnev, I. D.; Zhang, W. Nickel-Catalysed Asymmetric Hydrogenation of Oximes. *Nat. Chem.* **2022**, *14*, 920−927. (f) Wei, H.; Chen, H.; Chen, J.; Gridnev, I. D.; Zhang, W. Nickel-Catalyzed Asymmetric Hydrogenation of α-Substituted Vinylphosphonates and Diarylvinylphosphine Oxides. *Angew. Chem., Int. Ed.* **2023**, *62*, No. e202214990. (g) Li, B.; Wang, Z.; Luo, Y.; Wei, H.; Chen, J.; Liu, D.; Zhang, W. Nickel-Catalyzed Asymmetric Hydrogenation for the Preparation of α-Substituted Propionic Acids. *Nat. Commun.* **2024**, *15*, 5482.

(15) Selected papers: (a) Zhao, Y.; Ding, Y.-X.; Wu, B.; Zhou, Y.-G. Nickel-Catalyzed Asymmetric Hydrogenation for Kinetic Resolution of [2.2]Paracyclophane-Derived Cyclic *N*-Sulfonylimines. *J. Org. Chem.* **2021**, *86*, 10788−10798. (b) Deng, C.-Q.; Liu, J.; Luo, J.-H.;

https://doi.org/10.1021/jacs.4c10623
J. Am. Chem. Soc. XXXX, XXX, XXX−XXX

Gan, L.-J.; Deng, J.; Fu, Y. Proton-Promoted Nickel-Catalyzed Asymmetric Hydrogenation of Aliphatic Ketoacids. *Angew. Chem., Int. Ed.* **2022**, *61*, No. e202115983. (c) Xiao, G.; Xie, C.; Guo, Q.; Zi, G.; Hou, G.; Huang, Y. Nickel-Catalyzed Asymmetric Hydrogenation of γ-Keto Acids, Esters, and Amides to Chiral γ-Lactones and γ-Hydroxy Acid Derivatives. *Org. Lett.* **2022**, *24*, 2722−2727. (d) Xiao, G.; Xie, C.; Guo, Q.; Zi, G.; Hou, G.; Huang, Y. Highly Enantioselective Ni-Catalyzed Asymmetric Hydrogenation of β,β-Disubstituted Acrylic Acids. *Org. Chem. Front.* **2022**, *9*, 4472−4477. (e) Sudhakaran, S.; Shinde, P. G.; Aratikatla, E. K.; Kaulage, S. H.; Rana, P.; Parit, R. S.; Kavale, D. S.; Senthilkumar, B.; Punji, B. Nickel-Catalyzed Asymmetric Hydrogenation for the Synthesis of a Key Intermediate of Sitagliptin. *Chem. Asian J.* **2022**, *17*, No. e202101208. (f) Wang, S.; Xie, C.; Zhu, Y.; Zi, G.; Zhang, Z.; Hou, G. Enantioselective Synthesis of Chiral Cyclic Hydrazines by Ni-Catalyzed Asymmetric Hydrogenation. *Org. Lett.* **2023**, *25*, 3644−3648. (g) Yang, X.; Liu, G.; Xiang, X.; Xie, D.; Han, J.; Han, Z.; Dong, X.-Q. Ni-Catalyzed Asymmetric Hydrogenation of α-Substituted α,β-Unsaturated Phosphine Oxides/Phosphonates/ Phosphoric Acids. *Org. Lett.* **2023**, *25*, 738−743.

(16) (a) Duan, Y.; Li, L.; Chen, M.-W.; Yu, C.-B.; Fan, H.-J.; Zhou, Y.-G. Homogenous Pd-Catalyzed Asymmetric Hydrogenation of Unprotected Indoles: Scope and Mechanistic Studies. *J. Am. Chem. Soc.* **2014**, *136*, 7688−7700. (b) Colomer, I.; Chamberlain, A. E. R.; Haughey, M. B.; Donohoe, T. J. Hexafluoroisopropanol as a highly versatile solvent. *Nat. Rev. Chem.* **2017**, *1*, 0088. (c) Tzouras, N. V.; Zorba, L. P.; Kaplanai, E.; Tsoureas, N.; Nelson, D. J.; Nolan, S. P.; Vougioukalakis, G. C. Hexafluoroisopropanol (HFIP) as a Multifunctional Agent in Gold-Catalyzed Cycloisomerizations and Sequential Transformations. *ACS Catal.* **2023**, *13*, 8845−8860.

https://doi.org/10.1021/jacs.4c10623
J. Am. Chem. Soc. XXXX, XXX, XXX−XXX